Eur. Phys. J. C (2016) 76:684
DOI 10.1140/epjc/s10052-016-4536-4

THE EUROPEAN PHYSICAL JOURNAL C

Regular Article - Theoretical Physics

Phenomenological MSSM in light of new 13 TeV LHC data

Kamila Kowalska[a]

Fakultät für Physik, TU Dortmund, Otto-Hahn-Str. 4, 44221 Dortmund, Germany

Received: 2 September 2016 / Accepted: 23 November 2016 / Published online: 10 December 2016

Abstract We present the first analysis of the p19MSSM with neutralino dark matter, in light of 13 TeV LHC data with an integrated luminosity of ∼14/fb. We recast 12 experimental analyses performed by the ATLAS collaboration and derive exclusion bounds on the parameter space of the model. We find that 25% of the model points can be excluded at 95% C.L. by a combination of the implemented searches. The spectrum allowed after the 13 TeV results are taken into account presents stops heavier than at least 400 GeV, gluinos heavier than at least 790 GeV, and squarks of the first and second generation heavier than at least 440 GeV.

1 Introduction

In 2015 the LHC entered the second phase of its operation. The center-of-mass energy of the proton–proton collisions has increased to $\sqrt{s} = 13$ TeV. By now, both ATLAS and CMS collaborations have collected a large amount of data corresponding to an integrated luminosity of around 14/fb. The experimental analyses aimed at interpreting these results in the framework of Beyond-the-Standard Model (BSM) scenarios, including supersymmetry (SUSY), extra dimensions, leptoquarks, and many others. Albeit some of the searches present mild upward fluctuations in the number of signal events over the background yields, none of them has reached a statistical significance that would allow one to claim, or at least to suspect, the discovery of a new particle.

In this paper we study the impact of the new 13 TeV LHC data with luminosity of ∼14/fb on the phenomenological Minimal Supersymmetric Standard Model (pMSSM) [1] characterized by 19 independent parameters. To this end, we use a sample of model points generated by the ATLAS collaboration in Ref. [2] that satisfies a set of experimental constraints from dark matter searches, Higgs measurements, electroweak and flavor physics, as well as includes the exclusion bounds from the 8 TeV LHC SUSY searches. The previous LHC study of this dataset with $\sqrt{s} = 13$ TeV and luminosity of 3.2/fb has been performed in Ref. [3].

The model-dependent limits from the experimental SUSY searches are interpreted by the collaborations in the so-called Simplified Model scenarios (SMS) [4], which make simplifying assumptions as regards the masses of the SUSY particles. In most scenarios the SMS spectrum consists of only several light states, one of them being the lightest neutralino. If, however, also other light particles are present, the derived exclusion limits can be altered. Therefore, in order to evaluate in a complete and self-consistent way the impact of the LHC SUSY searches on the parameter space of p19MSSM, we reinterpret the SMS results by simulating in detail the experimental searches with a likelihood function approach [5–7].

This paper is organized as follows. In Sect. 2 we describe the model sample used in the study and make a brief overview of the numerical tools and procedures used to implement the LHC SUSY searches. Section 3 is dedicated to a discussion of our main results. We summarize our findings in Sect. 4.

2 Methodology

2.1 p19MSSM ATLAS sample

The phenomenological MSSM is characterized by 19 independent SUSY parameters defined at the scale $M_{\rm SUSY}$, which is the geometrical average of the physical stop masses. The number of free parameters results from the following assumptions: R-parity is conserved, all soft parameters are real, the off-diagonal elements of soft matrices are set to zero in order to ensure Minimal Flavor Violation, neutralino is the lightest supersymmetric particle (LSP), and two first generations of squarks and leptons are degenerate in order to suppress potentially large SUSY contributions to the flavor changing neutral currents processes.

[a] e-mail: kamila.kowalska@tu-dortmund.de

In this study we use a sample of p19MSSM model points provided by the ATLAS collaboration in Ref. [2] and generated using methods similar to those described in [1,8–10]. All masses and trilinear couplings where scanned up to 4 TeV, which results in the range of superpartner masses that falls within the reach of the LHC. The only exception was the trilinear coupling A_t, scanned up to 8 TeV in order to boost the Higgs boson mass to 125 GeV through the stop loops. The lower bounds imposed on the soft masses came from the direct SUSY searches at LEP [11]. The Standard Model parameters were fixed at their central values given in Ref. [12].

Additional phenomenological constraints from the dark matter (DM) searches (relic density, spin independent nucleon cross section, spin dependent proton cross sections), flavor physics (BR $(\mathrm{b} \to \mathrm{s}\gamma)$, BR $\left(\mathrm{B_s} \to \mu^+\mu^-\right)$, BR$(\mathrm{B_u} \to \tau\nu)$, $\delta\,(g-2)_\mu^{\mathrm{SUSY}}$) and the electroweak precision data ($\Delta\rho$) were also taken into account, with the acceptance ranges given in Table 1. Finally, the impact of 22 ATLAS SUSY searches at $\sqrt{s} = 7$ and 8 TeV with integrated luminosity of 20.3/fb was evaluated. The resulting p19MSSM sample contains 183,030 allowed model points. 33.5% of them is characterized by bino-like LSP, 42.6% by higgsino-like LSP, and 23.9% are the points for which the neutralino LSP is a wino. Note that the type of neutralino LSP has been defined by ATLAS according to the maximal neutralino mixing matrix parameter. As a consequence, not all the points in a given type of sample are pure gaugino eigenstates.

The lightest squarks and gluinos allowed by the 8 TeV data correspond to the compressed spectra region which is notoriously difficult to probe at the LHC. The reason is a small mass difference between the color sparticles and the lightest neutralino that results in very soft decay products. In fact, if this mass difference is very small, the next-to-LSP particle becomes semi-stable and cannot be tested by the standard SUSY searches. For this reason, following the approach of [2], we remove 3500 of such models from the sample. After that, the minimal masses of squarks and gluinos found in the p19MSSM set, together with the corresponding LSP mass, read

$$\begin{aligned}
m_{\tilde{t}_1}^{\min} &= 275\,\mathrm{GeV}, \quad m_{\tilde{\chi}_1^0} = 243\,\mathrm{GeV},\\
m_{\tilde{b}_1}^{\min} &= 234\,\mathrm{GeV}, \quad m_{\tilde{\chi}_1^0} = 220\,\mathrm{GeV},\\
m_{\tilde{d}_R}^{\min} &= 291\,\mathrm{GeV}, \quad m_{\tilde{\chi}_1^0} = 272\,\mathrm{GeV},\\
m_{\tilde{u}_R}^{\min} &= 251\,\mathrm{GeV}, \quad m_{\tilde{\chi}_1^0} = 222\,\mathrm{GeV},\\
m_{\tilde{u},\tilde{d}_L}^{\min} &= 302\,\mathrm{GeV}, \quad m_{\tilde{\chi}_1^0} = 266\,\mathrm{GeV},\\
m_{\tilde{g}}^{\min} &= 566\,\mathrm{GeV}, \quad m_{\tilde{\chi}_1^0} = 513\,\mathrm{GeV}.
\end{aligned} \tag{1}$$

On the other hand, in the region of the parameter space where neutralino LSP is light ($m_{\tilde{\chi}_1^0} \leq 50\,\mathrm{GeV}$) and sensitivity of the LHC SUSY searches reaches its maximum, the limits become significantly stronger and the minimal masses read

$$\begin{aligned}
m_{\tilde{t}_1}^{0} &= 553\,\mathrm{GeV}, \quad m_{\tilde{b}_1}^{0} = 498\,\mathrm{GeV},\\
m_{\tilde{d}_R}^{0} &= 633\,\mathrm{GeV}, \quad m_{\tilde{u}_R}^{0} = 739\,\mathrm{GeV},\\
m_{\tilde{g}}^{0} &= 1188\,\mathrm{GeV}.
\end{aligned} \tag{2}$$

2.2 13 TeV LHC SUSY searches

Both ATLAS and CMS collaborations performed a large number of analyses at $\sqrt{s} = 13\,\mathrm{TeV}$ that cover a wide spectrum of experimental signatures. For the purpose of this paper, we decided to implement the ATLAS searches only, in order to be consistent with the results of the 8 TeV analyses incorporated in the p19MSSM sample described in the previous subsection.

From 11 3.2/fb ATLAS searches within the R-parity conserving MSSM for which the experimental analysis are available, we implemented seven which exhibit both the strongest exclusion limits for a given production scenario and the largest expected sensitivity in beyond the SMS framework. We used here as a helpful guideline the results of Ref. [3] where the impact of six ATLAS searches on the same p19MSSM sample has been quantified. Five of the above analyses have been recently updated with 13–14/fb of data. Additionally, one 13.3/fb study appeared that does not have the lower luminosity equivalent. Below we present the full list of the implemented analyses:

Table 1 The lower and upper bounds on the relevant phenomenological observables as used in Ref. [2]

Constraint	Min	Max	Refs. (exp., theo.)
Ωh^2	–	0.1208	[13]
$\sigma_p^{\mathrm{SI}}, \sigma_p^{\mathrm{SD}}$	–	See Ref. [2]	[14–16]
$\Delta\rho$	−0.0005	0.0017	[17]
BR $(\mathrm{b} \to \mathrm{s}\gamma)$	2.69×10^{-4}	3.87×10^{-4}	[18]
BR $\left(\mathrm{B_s} \to \mu^+\mu^-\right)$	1.6×10^{-9}	4.2×10^{-9}	[19,20]
BR $(\mathrm{B_u} \to \tau\nu)$	6.6×10^{-5}	16.1×10^{-5}	[21–25]
$\delta\,(g-2)_\mu^{\mathrm{SUSY}}$	-17.7×10^{-10}	43.8×10^{-10}	[26–31]
m_h	124 GeV	128 GeV	[32,33]

– 0 leptons + 2–6 jets + E_T^{miss}, 3.2/fb [34], 13.3/fb [35],
– 1 lepton + jets + E_T^{miss}, 3.2/fb [36], 14.8/fb [37],
– 3 b-tagged jets + E_T^{miss}, 3.2/fb [38], 14.8/fb [39],
– 0 lepton + (b)jets + E_T^{miss}, 13.3/fb [40],
– 1 lepton + (b)jets + E_T^{miss}, 3.2/fb [41], 13.3/fb [42],
– 2 leptons + jets + E_T^{miss}, 3.2/fb [43],
– 2 b-tagged jets + E_T^{miss}, 3.2/fb [44],
– monojet + E_T^{miss}, 3.2/fb [45].

New results from the LHC 13 TeV are taken into account by employing the recast procedure developed and described in detail in Refs. [5–7]. Its key element is a construction of an approximate but accurate likelihood function, which yields an exclusion C.L. (confidence level) for each point in the analyzed p19MSSM sample.

In order to obtain the likelihood function, one needs to mimic the analyses performed by the experimental collaborations. For every point in the parameter space the spectrum is generated with `softsusy` [46] and the decay branching ratios calculated with `SUSYHIT` [47] (alternatively, the provided SLHA spectrum file is used). Next, 2×10^4 events are generated at the parton level with `PYTHIA8` [48] and the hadronization products are passed to the fast detector simulator `DELPHES 3` [49] to reconstruct the physical objects. The ATLAS detector card is used, with the settings adjusted to those recommended by the experimental collaboration. The b-tagging algorithm used by `DELPHES 3` is tuned to match the corresponding efficiencies reported by ATLAS for the 13 TeV data [50].

The physical objects produced by the detector simulator are used to construct a set of kinematical variables proper of a given SUSY search and chosen to reduce the SM background by applying a series of the selection cuts. Finally, different kinematical bins i are defined and the efficiencies ε_i are evaluated as the fraction of events that pass all the cuts.

The number of signal events in a given bin is determined as $s_i = \varepsilon_i \times \sigma_{\text{LO}} \times \int L$, where $\int L$ is the integrated luminosity and σ_{LO} the leading order (LO) cross sections. We decided to use the LO cross section instead of the next-to-LO (NLO) one as a good compromise between the accuracy of the results and the fact how time-consuming their derivation is. The SUSY spectrum that arises in the framework of the p19MSSM is in general complex and different particles contribute to the total production cross section. In order to incorporate the NLO corrections in a consistent way, one should either decompose each model into various production channels and use the official values of the NLO + NLL cross sections provided by LHC SUSY Cross Section Working Group [51], or interface the whole package with a numerical tool that calculates the NLO cross section directly. On the other hand, we have checked in the framework of several SMS that when the LO cross section is used instead of the NLO one, the resulting exclusion bounds on the sparticle mass are weakened by around 50–100 GeV in the part of the parameter space where the neutralino is light. Since the recast procedure employed in this study is designed as an approximation of the experimental analyses, we treat underestimation of the total cross section as an additional source of uncertainty and interpret our exclusion limits as conservative ones.

The signal is statistically compared to the numbers of the observed (o_i) and background (b_i) events, given in the experimental papers, through the Poisson distribution P. The systematic uncertainties on the background yields (δb_i) are taken into account by convolving P with the Gaussian distribution G. The likelihood function for each bin is thus calculated to be

$$\mathcal{L}_i(o_i, s_i, b_i) = \int P(o_i|s_i, \bar{b}_i) G(\bar{b}_i|b_i, \delta b_i) \mathrm{d}\bar{b}_i \,. \tag{3}$$

The total likelihood function $\mathcal{L}_{\text{LHC}}$ for a given model point is calculated either as a product of the likelihoods from each signal bin, or as the likelihood from the bin with the best expected sensitivity, depending on whether the bins are exclusive or inclusive. The appropriate exclusion C.L. is obtained from the $\delta\chi^2$ variable as $\delta\chi^2 = -2\log(\mathcal{L}_{\text{LHC}}/\mathcal{L}_0)$, where $\mathcal{L}_0$ corresponds to the background-only hypothesis.

Note that when the observed number of events is large enough, this approach is bound to give exactly the same results as the CL$_s$ method [52] employed by the experimental collaborations in order to derive the C.L. intervals. This is a direct consequence of the central limit theorem, which roughly states that if the data is independent its distribution will converge to the normal distribution in the limit of high statistics. The validity of this simplification should be verified case by case with the proper validation of the results. In practice, however, at the level of precision expected for analyses like this, no significant discrepancies between the two approaches can be registered for the number of observed and background events reported in the SUSY searches.

A brief description of each implemented ATLAS search, as well as validations of the recast procedure against the experimental results, is given in Appendix A.

3 Results for SUSY spectra

In this section we analyze the impact of the implemented ATLAS searches on the p19MSSM parameter space allowed after inclusion of the 8 TeV run data. Since no statistically significant excess above the SM background expectation is observed, we derive the exclusion limits only.

In Table 2 we show the percentage of model points that have been excluded at 95% C.L. by each of the implemented searches. To capture the dependence of the exclusion

Table 2 Percentage of the p19MSSM points that are excluded by 13 TeV searches at 95% C.L.. The results for bino-, higgsino-, and wino-like neutralino LSP, as well as for the whole p19MSSM sample, are presented in the consecutive columns

Search	Bino (%)	Higgsino (%)	Wino (%)	ALL (%)
3.2/fb				
0 leptons + 2–6 jets + E_T^{miss}	17.9	10.3	8.0	12.3
1 lepton + jets + E_T^{miss}	0.9	1.0	0.4	0.8
3 b-tagged jets + E_T^{miss}	2.4	3.2	1.0	2.4
1 lepton + (b)jets + E_T^{miss}	0.4	0.3	0.1	0.3
2 leptons + jets + E_T^{miss}	0.1	0.2	0.1	0.1
2 b-tagged jets + E_T^{miss}	1.3	0.3	0.3	0.6
Monojet + E_T^{miss}	2.6	0.1	0.3	1.0
Total 3.2/fb	19.8	12.3	8.6	14.5
∼14/fb				
0 leptons + 2–6 jets + E_T^{miss}	30.6	15.6	10.3	18.6
1 lepton + jets + E_T^{miss}	7.2	11.3	2.9	7.7
3 b-tagged jets + E_T^{miss}	3.4	5.0	1.4	3.5
1 lepton + (b)jets + E_T^{miss}	3.1	6.0	1.2	3.8
0 lepton + (b)jets + E_T^{miss}	5.6	4.5	1.4	4.1
Total ∼14/fb	34.8	25.5	13.5	24.7

bounds on the properties of the neutralino LSP, we present the results for the bino-, higgsino-, and wino-like LSP cases separately. In the last column of Table 2 the results for the whole p19MSSM sample are indicated. To quantify the total impact of the LHC 13 TeV data, we combine the individual searches through "the-best-of" strategy, using for each model point the result from the search that presents the best sensitivity.

Only 14.5% of the p19MSSM models can be excluded at 95% C.L. by the LHC SUSY searches with 3.2/fb of the 13 TeV data. The percentage increases to 19.8% if only bino-like LSP is taken into account, while for the higgsino-like LSP it is reduced to 12.3%. Those numbers are consistent with findings of Ref. [3] and we will make a more detailed comparison of the two sets of results later on. A difference in sensitivity of the LHC searches for different types of the LSP comes from the fact that the number of models with gluinos lighter than 1 TeV is much higher in the bino-like case than in the higgsino-like one, as already noted in Ref. [3]. That is due to the fact that if the LSP is bino-like, an efficient mechanism of co-annihilation must exist that allows one to reduce the relic density of the dark matter below the critical value, to avoid overclosing the universe. Indeed, almost all light gluinos find in the p19MSSM sample are very close in mass to the neutralino LSP.

In the case of wino-like neutralino LSP, we find that only 8.6% of the parameter space is excluded with the luminosity of 3.2/fb. That result is by a factor of 1.7 lower than the corresponding number quoted in Ref. [3]. Since such a reduction in sensitivity is observed for all the searches that were also considered in Ref. [3], a discrepancy most likely arises at the level of events generation.[1]

The most effective in setting the exclusion bounds are inclusive all-hadronic searches, both with b-tagged and non-b-tagged jets. The former shows perfect agreement with the results of Ref. [3] (except when the LSP is wino-like). In the case of the latter, the percentage of excluded models calculated by us is lower than the ones of Ref. [3] by around 25%. This discrepancy may result from a different tuning of the b-tagging algorithm used by DELPHES 3.

Contrarily, with 3.2/fb of data the 1 lepton searches can test only a small fraction of the parameter space, as in the p19MSSM the branching ratio for the color particles decaying to chargino (which would lead to a leptonicaly decaying W boson) is much smaller than the one directly to the LSP. Once more, our results are in agreement with the findings of Ref. [3].

The monojet analysis tests the region of the compressed spectra, mainly through the production of the first- and second-generation squarks. The efficiency of this search in our study is slightly lower than the one observed in Ref. [3], although one needs to keep in mind that this kind of analysis, being based on the initial state radiation jet identification, is particularly sensitive to the detector simulator settings.

Finally, in the case of the 2 lepton search its sensitivity over the p19MSSM parameter space is minimal. For this reason we do not include it in the higher luminosity update.

[1] Ref. [3] uses MadGraph5 to generate events and PYTHIA 6.428 for showering and hadronization.

The sensitivity of the LHC SUSY searches based on the ∼14/fb data sample is much stronger. After their inclusion 25.0% of the p19MSSM model points are excluded at 95% C.L.. For the bino-like LSP the corresponding number increases to almost 35%, while for the higgsino- and wino-like LSP 25.5 and 13.5% of the parameter space is excluded, respectively.

The improvement is particularly visible in the case of the 1 lepton + jets search, which is also confirmed by the ALTAS limits derived in the SMS framework. Such a significant increase of its reach results from the fact that a $\sim 2\sigma$ excess, observed in the 3.2/fb data in one of the kinematical bins proper to this search, is now gone. Contrarily, new all-hadronic analyses, in particular the one looking for 3 b jets signature, although exclude more models than their 3.2/fb counterparts, gained less in terms of sensitivity due to the presence of several $\sim 2\sigma$ excesses that weaken the observed exclusions limits with respect to the expected ones.

To get some qualitative feeling how the new LHC results affect the allowed mass ranges of the SUSY particles, we present their impact in two-dimensional projections of the full p19MSSM parameter space, following the style adopted in Ref. [2]. For each projection we bin the relevant sparticle masses, and for each bin we calculate the fraction of excluded models, defined as a ratio of the number of points excluded to the total number of points in a bin.

In Fig. 1 we show the percentage of p19MSSM models that are excluded at 95% C.L. by "the-best-of" combination of the 13 TeV SUSY searches with 3.2/fb and ∼14/fb of data in (a) $(m_{\tilde{g}}, m_{\tilde{\chi}_1^0})$ plane, in (b) $(m_{\tilde{d}_L}, m_{\tilde{\chi}_1^0})$ plane, in (c) $(m_{\tilde{d}_R}, m_{\tilde{\chi}_1^0})$ plane, and in (d) $(m_{\tilde{u}_R}, m_{\tilde{\chi}_1^0})$ plane. In gray those mass bins are shown that has been excluded already at 8 TeV. Red color indicates those parts of the parameter space where 100% of points is excluded and therefore can be interpreted as a 95% C.L. lower bound on the sparticle mass.

One observes that the strongest and most solid exclusion limits can be derived in the case of the gluino mass, which reads $m_{\tilde{g}} \gtrsim 1.45\,\text{TeV}$ if neutralino is light ($m_{\tilde{\chi}_1^0} \leq 50$ GeV), and $m_{\tilde{g}} \gtrsim 0.8\,\text{TeV}$ in the whole p19MSSM sample. The 95% C.L. exclusion bound coincide with the one derived in the framework of the SMS of Ref. [35] in the heavy neutralino region, while is weaker by around 300 GeV in the light neutralino region. This is due to the fact that inclusive all hadronic searches, being sensitive to the number and energy of the outgoing jets only, can test a wide variety of possible decay chains and produce similar results both in the framework of the SMS and within the more general SUSY scenarios.

In the case of the squarks of the first and second generations the exclusion limits are notably weaker than in the corresponding SMS of Ref. [35]. The main reason is that all eight suqarks are assumed to be degenerate in the SMS, while in the p19MSSM various mass hierarchies between the left- and right-handed superparters are possible. Figure 1 emphasizes also the difference in sensitivity of the SUSY searches when left and right squarks are considered. The reason is well known and was explained, for instance, in Ref. [2]. Since the left-handed squarks are close in mass their production cross section is always enhanced w.r.t. the right-handed ones. Moreover, since there are fewer valence down quarks than up in the proton, the limit of Fig. 1c is slightly weaker than the limit of Fig. 1d.

In Fig. 2 we show the percentage of p19MSSM models that are excluded at 95% C.L. in (a) $(m_{\tilde{t}_1}, m_{\tilde{\chi}_1^0})$ and (b) $(m_{\tilde{b}_1}, m_{\tilde{\chi}_1^0})$ planes. Contrarily to the case of gluino and squarks of the first and second generations, only a slight improvement with respect to the 8 TeV results is observed in the limits on the stop mass, mainly in the part of the parameter space were neutralino is relatively heavy. Dedicated 0 and 1 lepton searches, while effective in the framework of the SMS with right stops and neutralinos only, lose sensitivity if a larger number of light particles is present, or if different amounts of mixing between two stops are considered. On the other hand, the compressed spectra region is well tested by the monojet analysis.

The 13 TeV limit on the sbottom mass is by around 50 GeV stronger with respect to the 8 TeV results in the part of the parameter space where neutralino is lighter than 300 GeV. The improvement reaches 100 GeV in the compressed spectra region. Sbottoms are predominantly excluded by a combination of a dedicated 2 b jets search with 3.2/fb of data, and the all-hadronic multijet search with 13.3/fb, as both of them effectively test decay topologies characterized by the presence of 2 jets. When the former analysis is updated to higher luminosity, the exclusion limits should become even stronger.

We conclude this section with quoting the minimal values of superparticle masses left in the p19MSSM sample after the 95% C.L. exclusion bounds from the LHC 13 TeV have been imposed:

$$
\begin{aligned}
m^{\text{min}}_{\tilde{t}_1} &= 396\,\text{GeV}, \quad m_{\tilde{\chi}_1^0} = 376\,\text{GeV},\\
m^{0}_{\tilde{t}_1} &= 744\,\text{GeV}, \quad m_{\tilde{\chi}_1^0} < 50\,\text{GeV},\\
m^{\text{min}}_{\tilde{b}_1} &= 357\,\text{GeV}, \quad m_{\tilde{\chi}_1^0} = 342\,\text{GeV},\\
m^{0}_{\tilde{b}_1} &= 648\,\text{GeV}, \quad m_{\tilde{\chi}_1^0} < 50\,\text{GeV},\\
m^{\text{min}}_{\tilde{d}_L} &= 483\,\text{GeV}, \quad m_{\tilde{\chi}_1^0} = 439\,\text{GeV},\\
m^{0}_{\tilde{d}_L} &= 1064\,\text{GeV}, \quad m_{\tilde{\chi}_1^0} < 50\,\text{GeV},\\
m^{\text{min}}_{\tilde{d}_R} &= 439\,\text{GeV}, \quad m_{\tilde{\chi}_1^0} = 418\,\text{GeV},\\
m^{0}_{\tilde{d}_R} &= 726\,\text{GeV}, \quad m_{\tilde{\chi}_1^0} < 50\,\text{GeV},\\
m^{\text{min}}_{\tilde{u}_L} &= 477\,\text{GeV}, \quad m_{\tilde{\chi}_1^0} = 440\,\text{GeV},
\end{aligned}
$$

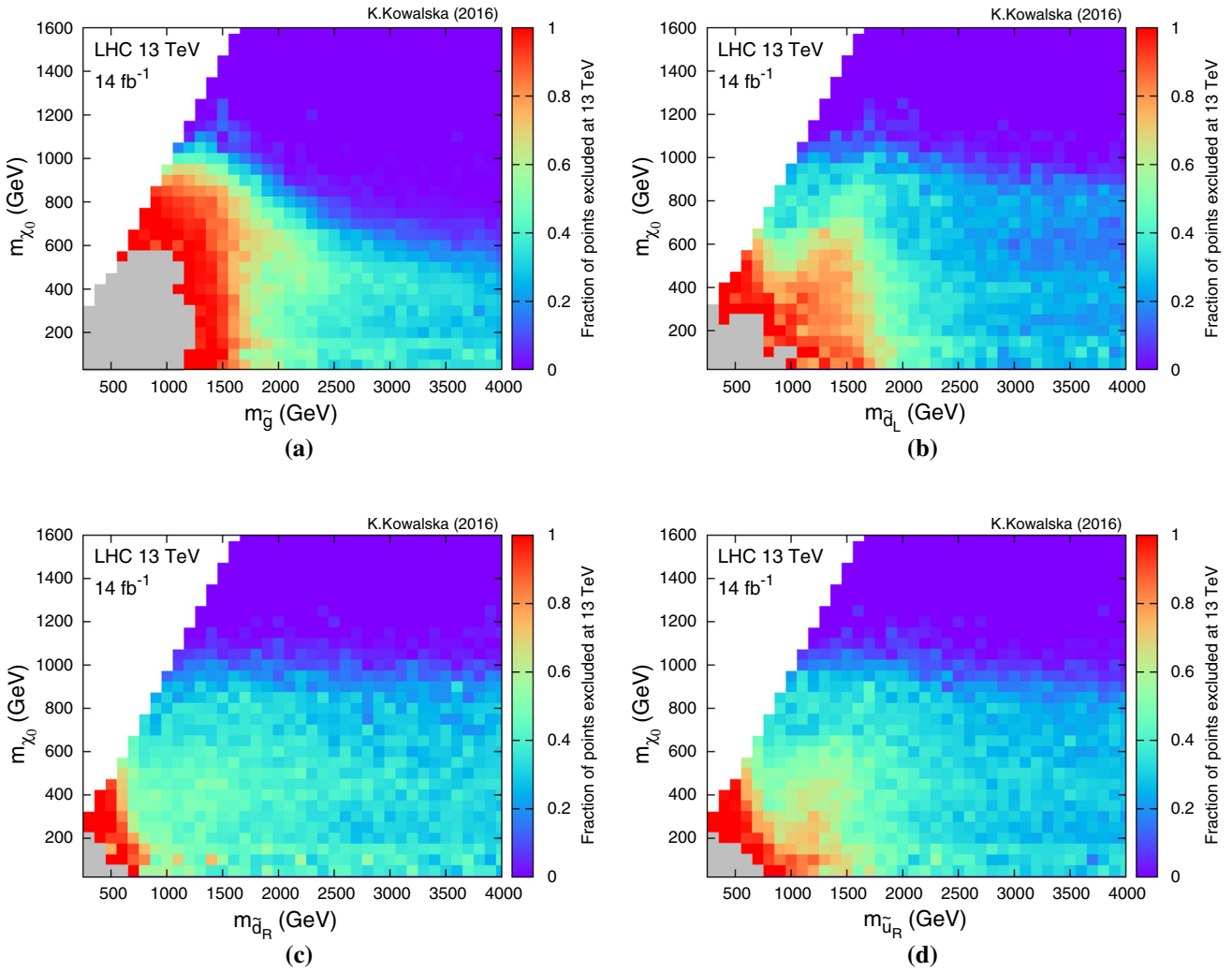

Fig. 1 Percentage of p19MSSM points excluded at 95% C.L. by a combination of 12 13 TeV ATLAS SUSY searches projected into **a** $(m_{\tilde{g}}, m_{\tilde{\chi}_1^0})$ plane, **b** $(m_{\tilde{d}_L}, m_{\tilde{\chi}_1^0})$ plane, **c** $(m_{\tilde{d}_R}, m_{\tilde{\chi}_1^0})$ plane, and **d** $(m_{\tilde{u}_R}, m_{\tilde{\chi}_1^0})$ plane. While combining the individual searches, "the-best-of" strategy is employed that uses for each model point the exclusion likelihood from the search with the best sensitivity. *Red color* indicates those parts of the parameter space where 100% of points is excluded. *Gray color* corresponds to masses that have been excluded by a combination of 22 ATLAS SUSY searches at 8 TeV

$$
\begin{aligned}
m^0_{\tilde{u}_L} &= 1061\,\text{GeV}, \quad m_{\tilde{\chi}_1^0} < 50\,\text{GeV},\\
m^{\min}_{\tilde{u}_R} &= 456\,\text{GeV}, \quad m_{\tilde{\chi}_1^0} = 323\,\text{GeV},\\
m^0_{\tilde{u}_R} &= 902\,\text{GeV}, \quad m_{\tilde{\chi}_1^0} < 50\,\text{GeV},\\
m_{\tilde{g}}{}^{\min} &= 792\,\text{GeV}, \quad m_{\tilde{\chi}_1^0} = 661\,\text{GeV},\\
m_{\tilde{g}}{}^0 &= 1452\,\text{GeV}, \quad m_{\tilde{\chi}_1^0} < 50\,\text{GeV}.
\end{aligned} \tag{4}
$$

When comparing to the 8 TeV results one can notice that the minimal allowed gluino mass has increased by approximately 300 GeV in the part of the parameter space where neutralino LSP is light, and by 250 GeV in the more compressed region. In the case of the squarks, the corresponding increase of the minimal allowed mass is lower, in the range of 50–200 GeV. One should bear in mind, however, that since our recast procedure is an accurate, yet still approximate, simulation of the experimental analysis, the precise values of the minimal masses given above should be treated with some caution.

4 Summary

In this paper we performed the first analysis of the p19MSSM in light of 13 TeV LHC data with integrated luminosity of ∼14/fb. We recast seven ATLAS SUSY searches based on the 3.2/fb data set and updated four of them, with the largest expected sensitivity, to incorporate new higher luminosity results.

We found that 25% of the p19MSSM parameter space that was phenomenologically allowed after inclusion of the 8 TeV

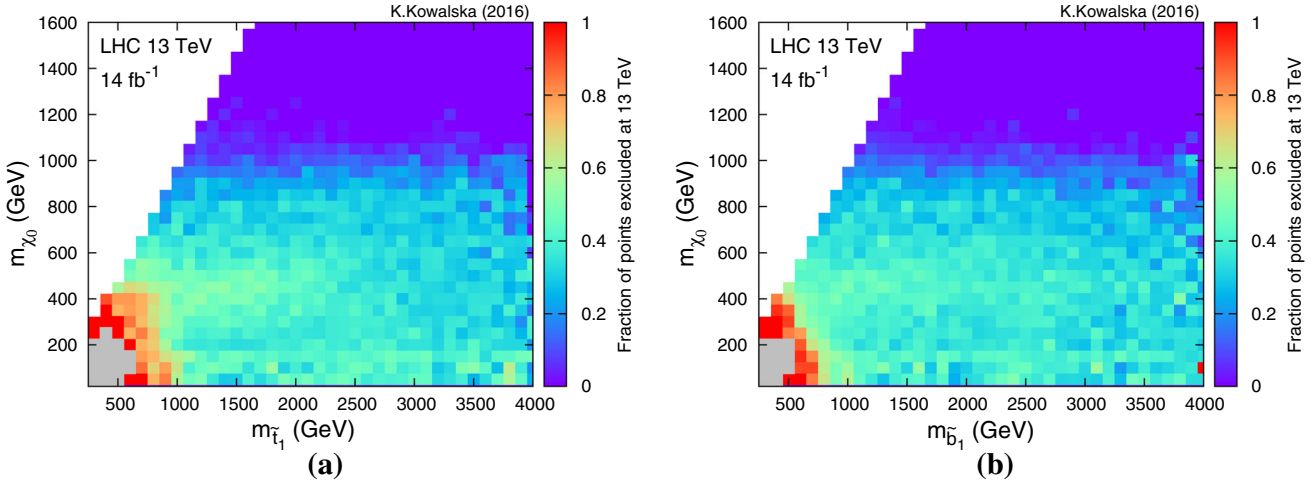

Fig. 2 Percentage of p19MSSM points excluded at 95% C.L. by a combination of 12 13 TeV ATLAS SUSY searches projected into **a** $(m_{\tilde{t}_1}, m_{\tilde{\chi}_1^0})$ plane, and **b** $(m_{\tilde{b}_1}, m_{\tilde{\chi}_1^0})$ plane. The color code is the same as in Fig. 1

data is now excluded at 95% C.L., predominantly through all-hadronic multijet searches. In the part of the parameter space where neutralino is lighter than 50 GeV, the lower limit on the gluino mass can be set at 1450 GeV, on the stop and sbottom masses at around 750 and 650 GeV, respectively, and on the left squark masses at 1060 GeV. In the compressed spectra region, which is notoriously difficult to test at the LHC as the decay products are soft, the new 95% C.L. exclusion bounds on the sparticle masses have reached approximately 790 GeV (gluinos), 400 GeV (stops), 350 GeV (sbottoms), and 470 GeV (left squarks).

Some of the experimental ATLAS analyses based on $\sim$14/fb of data reported moderate excesses in the number of signal events with respect to the SM background yields, reaching local significance of around $2-3\sigma$. One can hope these are harbingers of a future discovery. On the other hand, if none of the excesses turns into a SUSY signal when more data is collected, in the following months yet another chunk of the p19MSSM parameter space should be excluded by the LHC.

Acknowledgements I would like to thank Enrico Maria Sessolo for helpful discussions regarding the statistical treatment of the LHC limits. This project is supported in part by the DFG Research Unit FOR 1873 "Quark Flavour Physics and Effective Field Theories". The use of the CIS computer cluster at the National Centre for Nuclear Research in Warsaw is gratefully acknowledged.

A Implemented 13 TeV searches

In this appendix we present a summary of the implemented searches. We focus mainly on the consistency check between our recast and the official results by ATLAS. The technical details of each analysis can be found in the experimental papers. Note that in the validation analyses we used the NLO+NNL cross sections, provided by LHC SUSY Cross Section Working Group [51].

A.1 Search for squarks and gluinos in final states with jets and missing transverse momentum [34,35]

In this search a direct pair production of the gluinos and squark is analyzed. The experimental signature is composed of 2–6 hadronic jets and a large amount of missing energy. The analysis performs the following pre-selection cuts:

- lepton veto with $p_T > 10$ GeV,
- at least 2 jets with $p_T > 50$ GeV,
- $E_T^{\text{miss}} > 200$ GeV (3.2/fb), 250 GeV (13.3/fb).

Inclusive signal bins are defined for varying jet multiplicities and varying ranges of the following kinematical variables: the leading jets transverse momentum p_T(jet), the minimal azimuthal separation $(\Delta\phi(E_T^{\text{miss}}, \text{jet}))_{\text{min}}$, the ratio of missing energy and a scalar sum of jets transverse momenta $E_T^{\text{miss}}/\sqrt{H_T}$, and m_{eff}(incl) defined as the scalar sum of the transverse momenta of the jets with $p_T > 50$ GeV and E_T^{miss}. In Table 3 we show a cut flows comparison between the experimental analysis by ATLAS with 3.2/fb of data and the results of our recast, for a signal benchmark point $(m_{\tilde{g}}, m_{\tilde{\chi}_1^0}) = (1100, 700)$ GeV. The same comparison for a point $(m_{\tilde{q}}, m_{\tilde{\chi}_1^0}) = (1000, 400)$ GeV is shown in Table 4.

Table 3 Comparison of the cut flows for the signal point $(m_{\tilde{g}}, m_{\tilde{\chi}_1^0}) = (1100, 700)$ GeV in the 0 lepton + 2–6 jets + E_T^{miss} ATLAS 3.2/fb search and in the recast tool

Cuts	$E_T^{\text{miss}} > 200$ GeV, $p_T(\text{jet}_1)$	N_{jet} (%)	$(\Delta\phi(E_T^{\text{miss}}, \text{jet}))_{\text{min}}$ (%)	$p_T(\text{jet}_2)$ (%)	$E_T^{\text{miss}}/\sqrt{H_T}$ (%)	m_{eff}(incl) (%)
SR2: ATLAS	35.1	35.0	29.3	29.3	11.8	3.3
SR2: recast	36.5	36.5	29.8	29.7	11.6	4.8
SR5: ATLAS	57.7	26.8	20.0	19.7	5.1	1.5
SR5: recast	62.1	33.1	23.4	23.1	6.5	2.7

Table 4 Comparison of the cut flows for the signal point $(m_{\tilde{q}}, m_{\tilde{\chi}_1^0}) = (1000, 400)$ GeV in the 0 lepton + 2–6 jets + E_T^{miss} ATLAS 3.2/fb search and in the recast tool

Cuts	$E_T^{\text{miss}} > 200$ GeV, $p_T(\text{jet}_1)$	N_{jet} (%)	$(\Delta\phi(E_T^{\text{miss}}, \text{jet}))_{\text{min}}$ (%)	$p_T(\text{jet}_2)$ (%)	$E_T^{\text{miss}}/\sqrt{H_T}$ (%)	m_{eff}(incl) (%)
SR2: ATLAS	77.0	75.9	67.8	67.8	44.5	20.8
SR2: recast	77.6	77.6	68.6	67.8	45.3	22.5
SR3: ATLAS	84.8	83.5	66.1	49.3	19.6	3.8
SR3: recast	85.2	85.2	66.1	47.3	19.1	5.2

The signal regions are presented that provide the most stringent exclusion.

In Fig. 3a we present a validation of our simulation in terms of the exclusion limits in the parameter space of $(m_{\tilde{g}}, m_{\tilde{\chi}_1^0})$ for 3.2/fb analysis. Gray diamonds represent the points excluded by our likelihood function at the 99.7% C.L., cyan circles are excluded at the 95.0% C.L., and blue triangles are excluded at the 68.3% C.L. The points depicted as red squares are considered as allowed. The solid black line shows the 95% C.L. ATLAS exclusion limit, which we present for comparison. A corresponding validation in the $(m_{\tilde{q}}, m_{\tilde{\chi}_1^0})$ plane is shown in Fig. 3b. Validations of the 13.3 /fb analysis, for the same SMS, are shown in Fig. 3c, d.

A.2 Search for gluinos in events with an isolated lepton, jets and missing transverse momentum [36,37]

In this search a direct pair production of gluinos is assumed that undergo a three-body decay into 2 quarks and a chargino. The latter subsequently decays into neutralino LSP and the on/off-shell W boson. The experimental signature is characterized by presence of exactly 1 lepton, hadronic jets and large amount of missing energy. The analysis performs the following pre-selection cuts:

- one electron (muon) with $p_T > 7(6)$ GeV,
- at least 2 jets with $p_T > 30$ GeV.

The inclusive signal bins are defined for varying jet multiplicities, soft- and hard-lepton channels (with $p_T^l < 35$ GeV and $p_T^l \geq 35$, respectively) and varying ranges of the following kinematical variables: the leading jet's transverse momentum $p_T(\text{jet})$, the transverse mass m_T of the signal lepton and missing transverse momentum, sum of transverse momenta of all signal jets and the signal lepton H_T, and the effective mass m_{eff}(incl) defined as a sum over transverse momenta of E_T^{miss}, all signal jets and the lepton. In Table 5 we show a cut flows comparison between the experimental analysis by ATLAS with 3.2/fb of data and the results of our recast, for a signal benchmark point $(m_{\tilde{g}}, m_{\tilde{\chi}_1^\pm}, m_{\tilde{\chi}_1^0}) = (1385, 705, 25)$ GeV. In Fig. 4 we present a validation of our simulation in terms of the exclusion limits in the parameter space of $(m_{\tilde{g}}, m_{\tilde{\chi}_1^0})$. Figure 4a corresponds to the 3.2/fb analysis, while Fig. 4b to its 14.8/fb update. The color code is the same as in Fig. 3.

A.3 Search for pair production of gluinos decaying via stop and sbottom in events with b jets and large missing transverse momentum [38,39]

In this search a direct pair production of the gluinos is assumed which can then decay through the off-shell sbottoms and stops. The experimental signature is characterized by at least 3 energetic b-tagged jets and large amount of missing energy. The analysis performs the following pre-selection cuts:

- at least 4 signal jets with $p_T > 30$ GeV,
- at least 3 b jets with $p_T > 30$ GeV,
- $E_T^{\text{miss}} > 200$ GeV.

The following kinematical variables are used to discriminate between the signal and the background: the effective mass m_{eff}(incl) defined as a sum over transverse momenta of E_T^{miss}, all signal jets and leptons; its subclass $m_{\text{eff}}^{\text{4j}}$ which includes

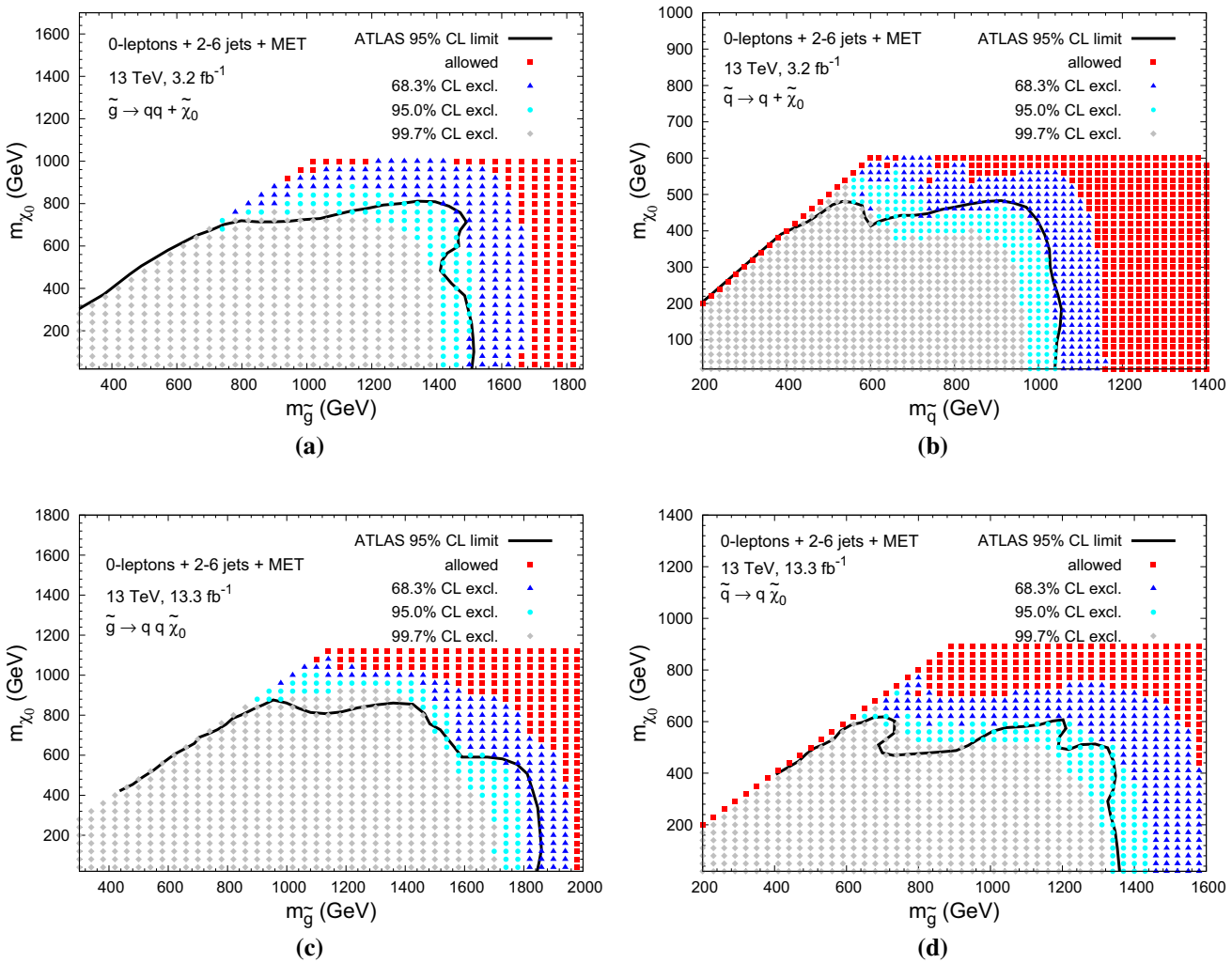

Fig. 3 **a** Our simulation of the ATLAS 0 lepton search with 3.2/fb of data for direct gluino production assuming a decay chain $\tilde{g} \to qq\tilde{\chi}_1^0$. **b** The same for direct squark production assuming a decay chain $\tilde{q} \to q\tilde{\chi}_1^0$. **c**, **d** The same for 13.3/fb analysis. Points that are excluded at the 99.7% C.L. are shown as *gray diamonds*, at the 95.0% C.L. as *cyan circles*, and at the 68.3% C.L. as *blue triangles*. The points shown as *red squares* are considered as allowed. The *solid black lines* show the published 95% C.L. contours by ATLAS

Table 5 Comparison of the cut flows for the signal point $(m_{\tilde{g}}, m_{\tilde{\chi}_1^\pm}, m_{\tilde{\chi}_1^0}) = (1385, 705, 25)$ GeV in the 1 lepton + jets + E_T^{miss} ATLAS 3.2/fb search and in the recast tool

Cuts	E_T^{miss} (%)	$p_T(\text{jet}_1)$ (%)	$p_T(\text{jet}_{\text{last}})$ (%)	m_T (%)	$E_T^{\text{miss}}/m_{\text{eff}}$(incl)	m_{eff}(incl) (%)
5-jet SR: ATLAS	19.2	18.2	16.0	8.5	8.3	7.6
5-jet SR: recast	18.2	17.4	15.3	9.6	9.5	8.3
6-jet SR: ATLAS	19.2	15.1	15.1	9.0	5.3	5.3
6-jet SR: recast	18.2	16.3	15.3	10.7	6.6	6.6
4-jet high-x SR: ATLAS	21.6	19.4	19.4	19.4	1.5	1.4
4-jet high-x SR: recast	19.7	16.5	16.5	16.5	2.8	2.3

4 leading jests only; the minimum transverse mass $m^b_{T,\text{min}}$ formed by missing energy and any of the 3 leading b-tagged jets; and the minimum azimuthal angle $\Delta\phi^{4j}_{\text{min}}$ between E_T^{miss} and the leading 4 jets.

For the sbottom-mediated decay model (denoted as Gbb) the inclusive signal regions are defined for varying ranges of missing energy and m^{4j}_{eff}. For the top-mediated decay model (denoted as Gtt) inclusive signal regions with no leptons

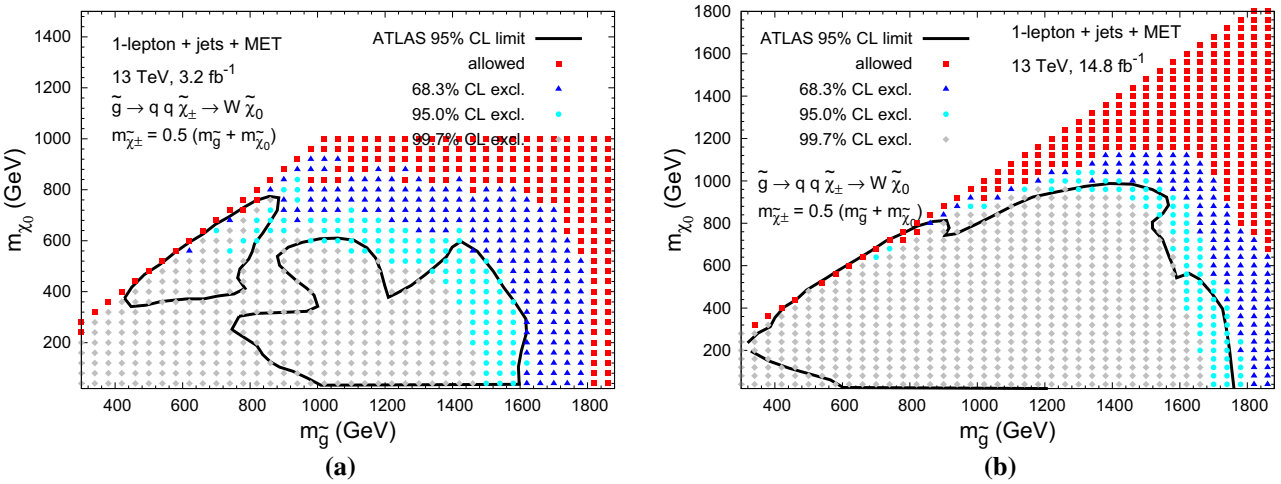

Fig. 4 **a** Our simulation of the ATLAS 1 lepton search in the 3.2/fb analysis for direct gluino production for the mass of chargino $m_{\tilde{\chi}_1^\pm} = \frac{1}{2}(m_{\tilde{g}} + m_{\tilde{\chi}_1^0})$. **b** The same for 14.8/fb analysis. The color code is the same as in Fig. 3

Table 6 Comparison of the cut flows for the signal point $(m_{\tilde{g}}, m_{\tilde{\chi}_1^0}) = (1700, 200)$ GeV in the 3 b jets + E_T^{miss} ATLAS 3.2/fb search and in the recast tool

Cuts	≥4 jets (%)	≥3 b jets (%)	$\Delta\phi_{\text{min}}^{\text{4j}}$ (%)	$m_{\text{eff}}^{\text{4j}}/m_{\text{eff}}$(incl) (%)	$E_T^{\text{miss}} > 350$ GeV (%)	p_T(jet) > 90 GeV(%)
Gbb-A: ATLAS	94.8	59.0	39.6	36.6	33.2	25.5
Gbb-A: recast	98.6	52.3	35.4	32.2	29.0	22.2
Gtt-0L-A: ATLAS	96.3	71.8	26.4	18.6	15.4	–
Gtt-0L-A: recast	99.9	68.3	28.0	20.1	16.6	–

and with 1 lepton are defined, differentiated by the values of E_T^{miss}, m_{eff}(incl), and the number of b-tagged jets.

In Table 6 we show a comparison of the cut flows between the experimental analysis by ATLAS with 3.2/fb of data and the results of our recast, for a signal benchmark point $(m_{\tilde{g}}, m_{\tilde{\chi}_1^0}) = (1700, 200)$ GeV. The signal regions with the best efficiency are presented. In Fig. 5a we show a validation of our simulation in terms of the exclusion limits in the parameter space of $(m_{\tilde{g}}, m_{\tilde{\chi}_1^0})$ for the Gbb model. A corresponding validation for the Gtt model is shown in Fig. 5b. Validations for the 14.8/fb analysis, for the same SMS, are shown in Fig. 5c, d. The color code is the same as in Fig. 3.

A.4 Search for supersymmetry in events containing a leptonically decaying Z boson, jets and missing transverse momentum [53]

In this search pair production of gluinos is assumed. The simplified model considered here assumes a three-body decay of the gluino into quarks and second neutralino, with a subsequent decay of the latter into a neutralino and Z boson (reconstructed from 2 leptons). The pre-selection cuts include:

- at least two signal jest with $p_T > 30$ GeV,
- at least two signal leptons with $p_T > 25$ GeV,
- the leading and subleading leptons form a same-flavor opposite-sign pair,
- $E_T^{\text{miss}} > 225$ GeV.

The following kinematical variables are used to discriminate between the signal and the background: the invariant mass m_{ll} of the dilepton system, and the sum of transverse momenta of all signal jets and two leading leptons H_T. Only one signal region is defined with $H_T > 600$ GeV and $81\,\text{GeV} < m_{ll} < 101\,\text{GeV}$.

In Fig. 6a we present a validation of our simulation in terms of the exclusion limits in the parameter space of $(m_{\tilde{g}}, m_{\tilde{\chi}_2^0})$. The color code is the same as in Fig. 3. For the second neutralino mass up to 400 GeV we obtain a very good agreement with the experimental bound. For larger values of $m_{\tilde{\chi}_2^0}$ a discrepancy is observed that reaches around 100 GeV for $m_{\tilde{\chi}_2^0} \sim 800$ GeV.

A.5 Search for top squarks in final states with 1 isolated lepton, jets, and missing transverse momentum [41,42]

In this search a light partner of the top quark is tested in two scenarios: gluino-mediated pair production of the stop with a

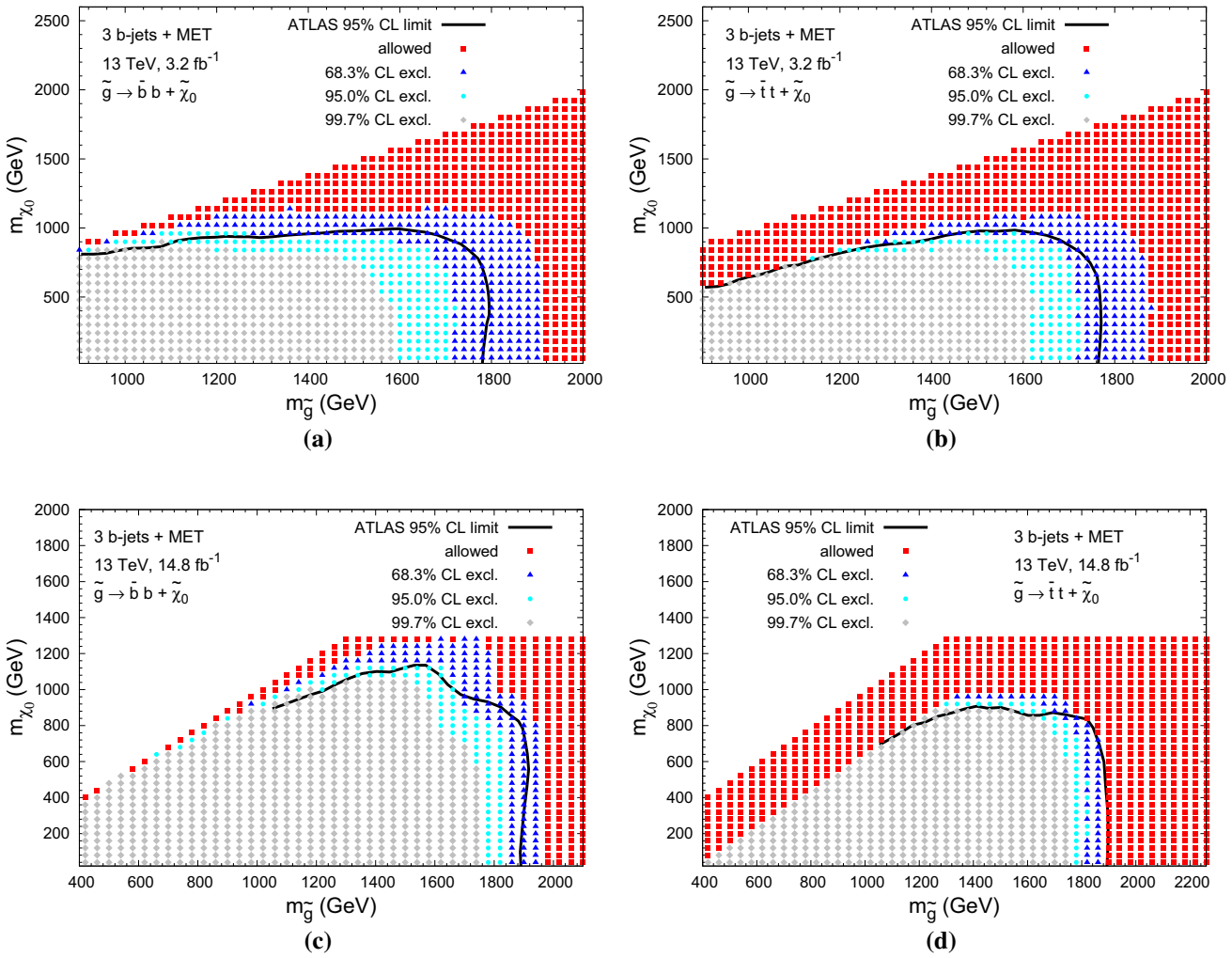

Fig. 5 **a** Our simulation of the ATLAS 3 b-tagged jets search with 3.2/fb of data for direct gluino production assuming a decay chain $\tilde{g} \to bb\tilde{\chi}_1^0$. **b** The same for a decay chain $\tilde{g} \to tt\tilde{\chi}_1^0$. **c**, **d** The same for the 14.8/fb analysis. The color code is the same as in Fig. 3

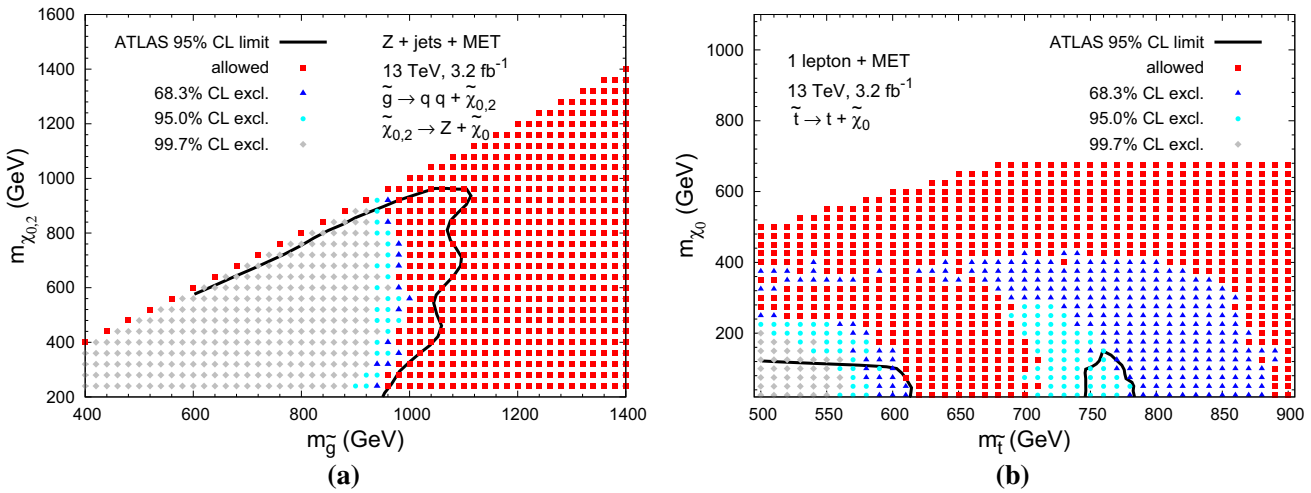

Fig. 6 **a** Our simulation of the ATLAS Z + jets search for direct gluino production. **b** The same for ATLAS 1 lepton search for direct stop production and a decay $\tilde{t}_1 \to t\tilde{\chi}_1^0$. Both validations correspond to 3.2/fb analyses. The color code is the same as in Fig. 3

small stop and neutralino LSP mass splitting, and direct pair production of the stops. The experimental signature includes 1 lepton, jets and large amount of missing energy. The analysis performs the following pre-selection cuts:

- exactly one signal lepton with $p_T > 25$ GeV,
- at least 4 signal jets with $p_T > 25$ GeV,
- $E_T^{\text{miss}} > 200$ GeV.

The following kinematical variables are used to discriminate between the signal and the background: azimuthal angle $\Delta\phi(E_T^{\text{miss}}, \text{jet})$ between 2 leading jets and missing energy, the transverse mass m_T of the signal lepton and missing transverse momentum, the asymmetric stransverse mass am_{T2}, the invariant mass m_{top}^{χ} of the 3 jets in the event most compatible with the hadronic decay products of a top quark, and the angular separation $\Delta R(b, l)$ between the signal lepton and the highest-p_T b jet.

The signal regions are defined to cover various decay topologies and kinematical regimes. In Table 7 we show a comparison of the cut flows between the experimental analysis by ATLAS with 3.2/fb of data and the results of our recast, for a signal benchmark point $(m_{\tilde{t}_1}, m_{\tilde{\chi}_1^0}) = (600, 260)$ GeV in the SR1 which is the most sensitive bin in this scenario.

In Fig. 6b we present a validation of our simulation in terms of the exclusion limits in the parameter space of $(m_{\tilde{t}_1}, m_{\tilde{\chi}_1^0})$ for the direct stop production scenario in the analysis based on 3.2/fb of data. A corresponding validation for the 13.2/fb search is shown in Fig. 7a. The color code is the same as in Fig. 3.

A.6 Search for the supersymmetric partner of the top quark in the jets plus missing energy final state [40]

In this search a pair production of the light partner of the top quark is tested. The experimental signature includes jets (two of which are tagged as originating from a b-quark) and large amount of missing energy. The analysis performs the following pre-selection cuts:

- lepton veto,
- at least 4 signal jets with $p_T > 40$ GeV,
- $E_T^{\text{miss}} > 250$ GeV.

The following kinematical variables are used to discriminate between the signal and the background: azimuthal angle $\Delta\phi(E_T^{\text{miss}}, \text{jet})$ between 2 leading jets and missing energy, the transverse mass m_T^b of the missing transverse momentum and the b-tagged jet closest in ϕ to p_T^{miss}, the angular separation $\Delta R(b, b)$ between 2 b-tagged jets, the ratio of missing energy and a scalar sum of jets transverse momenta $E_T^{\text{miss}}/\sqrt{H_T}$, and the mass $m_{\text{jet}, R=1.2}^{0,1}$ of the 2 leading jets reclustered with a distance parameter $R = 1.2$

Eleven signal regions are defined to target various kinematic regimes. In Fig. 7b we present a validation of our simulation in terms of the exclusion limits in the parameter space of $(m_{\tilde{t}_1}, m_{\tilde{\chi}_1^0})$ for the direct stop production scenario in the analysis based on the 13.2/fb of data. The SMS is tested in which stop decays via $\tilde{t}_1 \to t\tilde{\chi}_1^0$ or $\tilde{t}_1 \to bW\tilde{\chi}_1^0$, depending on kinematics. The color code is the same as in Fig. 3.

A.7 Search for direct top squark pair production in final states with 2 leptons [43]

In this search a pair production of the top squarks is assumed, decaying softly into chargino close in mass, $\tilde{t}_1 \to b\tilde{\chi}_1^{\pm}$, which then undergoes a decay $\tilde{\chi}_1^{\pm} \to W\tilde{\chi}_1^0$. The experimental signature is characterized by exactly two opposite charge leptons and large amount of missing energy. The analysis performs the following pre-selection cuts:

- leading lepton with $p_T > 25$ GeV and subleading lepton with $p_T > 15$ GeV,
- no other leptons with $p_T > 10$ GeV.

The following kinematical variables are used to discriminate between the signal and the background: the invariant mass of the 2 leptons m_{ll}, the leptonic stransverse mass m_{T2}, and the ratio $E_T^{\text{miss}}/m_{\text{eff}}(\text{incl})$, where $m_{\text{eff}}(\text{incl})$ is defined as the scalar sum of E_T^{miss} and the momenta of leptons and up to 2 jets with $p_T > 50$ GeV.

In the 3.2/fb analysis, two exclusive signal regions are defined, one for the same-flavor lepton pair, and the other for the opposite flavor lepton pair. The exclusion limit is derived as a statistical combination of the limits from both regions. In Fig. 8a we present a validation of our simulation in terms of the exclusion limits in the parameter space of $(m_{\tilde{t}_1}, m_{\tilde{\chi}_1^0})$, assuming $m_{\tilde{\chi}_1^{\pm}} = m_{\tilde{t}_1} - 10$ GeV.

A.8 Search for bottom squark pair production [44]

In this search a pair production of the bottom squarks is assumed. The experimental signature includes 2 b-tagged jets and large amount of missing energy. The analysis performs the following pre-selection cuts:

- lepton veto with $p_T > 10$ GeV,
- $E_T^{\text{miss}} > 250$ GeV.

The following kinematical variables are used to discriminate between the signal and the background: azimuthal angle $\Delta\phi(E_T^{\text{miss}}, \text{jet})$ between the leading jet and missing energy, the minimum azimuthal angle $\Delta\phi_{\text{min}}^{4\text{j}}$ between E_T^{miss} and the leading 4 jets, the invariant mass of the 2 b jets m_{bb}, the contransverse mass m_{CT}, and the effective mass $m_{\text{eff}}(\text{incl})$

Table 7 Comparison of the cut flows for the signal point $(m_{\tilde{t}_1}, m_{\tilde{\chi}_1^0}) = (600, 260)$ GeV in the 1 lepton + jets + E_T^{miss} ATLAS 3.2/fb search and in the recast tool

Cuts	1 lepton (%)	≥4 jets (%)	$\Delta\phi(E_T^{\text{miss}}, \text{jet})$ (%)	$p_T(\text{jet}_i)$ (%)	E_T^{miss} (%)	m_T (%)	am_{T2} (%)	m_{top}^{χ} (%)	$\Delta R(b, l)$ (%)
SR1: ATLAS	23.4	16.1	10.1	7.0	5.1	2.9	2.1	1.7	1.6
SR1: recast	20.2	15.3	8.9	6.0	4.3	2.9	2.6	1.9	1.8

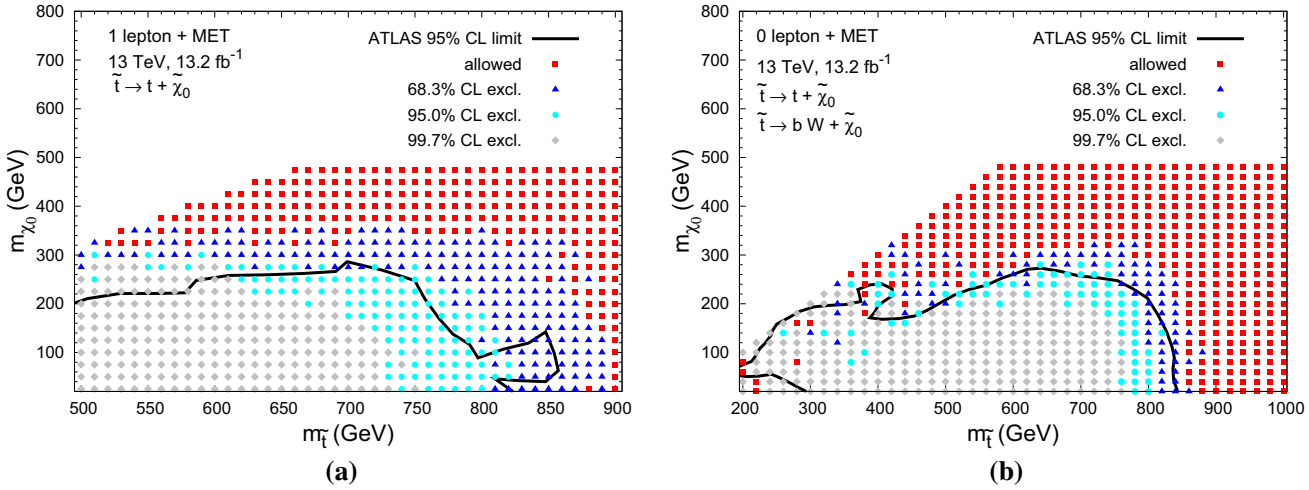

Fig. 7 **a** Our simulation of the ATLAS 1 lepton search with 13.2/fb of data for direct stop production and a decay $\tilde{t}_1 \to t\tilde{\chi}_1^0$. **b** The same for the corresponding ATLAS 0 lepton analysis. The color code is the same as in Fig. 3

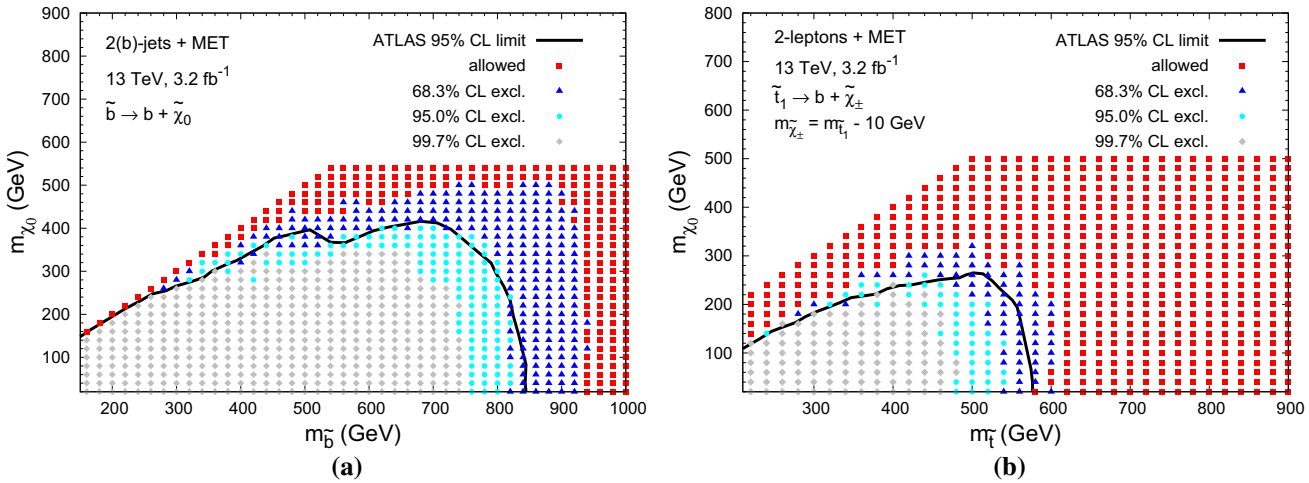

Fig. 8 **a** Our simulation of the ATLAS 2 lepton search for direct stop production. **b** The same for ATLAS 2 b jets search for direct sbottom production. The color code is the same as in Fig. 3

defined as the scalar sum of the E_T^{miss} and the momenta the 2 (3) leading jets.

Two signal regions are defined, characterized either by two energetic b jets or 2 b jets accompanied by an energetic jet from the initial state radiation. The exclusion limit is set based on the best SR at each point of the parameter space. In Fig. 8b we present a validation of our simulation in terms of the exclusion limits in the parameter space of $(m_{\tilde{b}_1}, m_{\tilde{\chi}_1^0})$.

A.9 Search for new phenomena in final states with an energetic jet and large missing transverse momentum [45]

In this search a pair production of squarks is assumed in compressed scenarios where the mass difference between squark and neutralino LSP is small. The experimental signature is characterized by an energetic jet originating from the ini-

Table 8 Comparison of the cut flows for the signal point $(m_{\tilde{t}_1}, m_{\tilde{\chi}_1^0}) = (350, 345)$ GeV in the monojet + E_T^{miss} ATLAS search and in the recast tool

Cuts	Lepton veto (%)	$N_{\text{jets}} \leq 4$ (%)	$p_T(\text{jet}_1) > 250$ GeV (%)	$E_T^{\text{miss}} > 250$ GeV (%)	E_T^{miss} (%)
EM1: ATLAS	79.9	74.5	17.8	16.2	3.2
EM1: recast	99.3	69.3	13.8	11.7	1.1

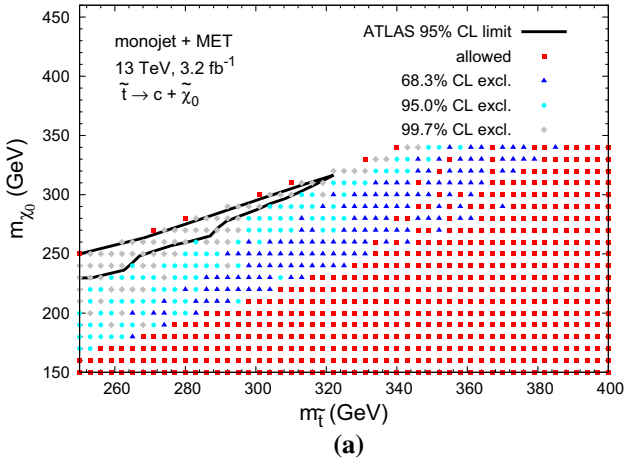

Fig. 9 **a** Our simulation of the ATLAS monojet search for direct stop production. The color code is the same as in Fig. 3

tial state radiation and large amount of missing energy. The analysis performs the following pre-selection cuts:

- leading jet with $p_T > 250$ GeV and$|\eta| < 2.4$,
- no more than 4 jets with $p_T > 30$ GeV,
- lepton veto.

Six exclusive signal bins are defined characterized uniquely by the amount of missing energy. In Table 8 we show a comparison of the cut flows between the experimental analysis by ATLAS and the results of our recast, for a signal benchmark point $(m_{\tilde{t}_1}, m_{\tilde{\chi}_1^0}) = (350, 345)$ GeV. In Fig. 9 we present a validation of our simulation in terms of the exclusion limit in the parameter space of $(m_{\tilde{t}_1}, m_{\tilde{\chi}_1^0})$. Note that, despite the fact that the experimental cuts employed in this search are relatively straightforward, our recast seems to exclude larger part of the parameter space that it was reported by ATLAS. Since the crucial element of the analysis is the correct identification of the initial state radiation jet, it emphasizes the importance of proper modeling of this phenomenon.

References

1. C.F. Berger, J.S. Gainer, J.L. Hewett, T.G. Rizzo, Supersymmetry without prejudice. JHEP **02**, 023 (2009). arXiv:0812.0980 [hep-ph]
2. ATLAS Collaboration, G. Aad et al., Summary of the ATLAS experiments sensitivity to supersymmetry after LHC Run 1 interpreted in the phenomenological MSSM. JHEP **10**, 134 (2015). arXiv:1508.06608 [hep-ex]
3. A. Barr, J. Liu, First interpretation of 13 TeV supersymmetry searches in the pMSSM. arXiv:1605.09502 [hep-ph]
4. CMS Collaboration, S. Chatrchyan et al., Interpretation of searches for supersymmetry with simplified models. Phys. Rev. D **88**(5), 052017 (2013). arXiv:1301.2175 [hep-ex]
5. A. Fowlie, M. Kazana, K. Kowalska, S. Munir, L. Roszkowski et al., The CMSSM favoring new territories: the impact of new LHC limits and a 125 GeV higgs. Phys. Rev. D **86**, 075010 (2012). arXiv:1206.0264 [hep-ph]
6. A. Fowlie, K. Kowalska, L. Roszkowski, E.M. Sessolo, Y.-L.S. Tsai, Dark matter and collider signatures of the MSSM. Phys. Rev. D **88**, 055012 (2013). arXiv:1306.1567 [hep-ph]
7. K. Kowalska, E.M. Sessolo, Natural MSSM after the LHC 8 TeV run. Phys. Rev. D **88**(7), 075001 (2013). arXiv:1307.5790 [hep-ph]
8. M.W. Cahill-Rowley, J.L. Hewett, S. Hoeche, A. Ismail, T.G. Rizzo, The new look pMSSM with neutralino and gravitino LSPs. Eur. Phys. J. C **72**, 2156 (2012). arXiv:1206.4321 [hep-ph]
9. M.W. Cahill-Rowley, J.L. Hewett, A. Ismail, T.G. Rizzo, More energy, more searches, but the phenomenological MSSM lives on. Phys. Rev. D **88**(3), 035002 (2013). arXiv:1211.1981 [hep-ph]
10. M. Cahill-Rowley, J.L. Hewett, A. Ismail, T.G. Rizzo, Lessons and prospects from the pMSSM after LHC Run I. Phys. Rev. D **91**(5), 055002 (2015). arXiv:1407.4130 [hep-ph]
11. The LEP SUSY Working Group and the ALEPH, DELPHI, L3 and OPAL experiments, note LEPSUSYWG/01-03.1. http://lepsusy.web.cern.ch/lepsusy
12. Particle Data Group Collaboration, K.A. Olive et al., Review of particle physics. Chin. Phys. C **38**, 090001 (2014)
13. Planck Collaboration, P.A.R. Ade et al., Planck 2015 results. XIII. Cosmological parameters. Astron. Astrophys. **594**, A13 (2016). arXiv:1502.01589 [astro-ph.CO]
14. LUX Collaboration, D.S. Akerib et al., First results from the LUX dark matter experiment at the Sanford Underground Research Facility. Phys. Rev. Lett. **112**, 091303 (2014). arXiv:1310.8214 [astro-ph.CO]
15. COUPP Collaboration, E. Behnke et al., First dark matter search results from a 4-kg CF_3I bubble chamber operated in a deep underground site. Phys. Rev. D **86**(5), 052001 (2012). arXiv:1204.3094 [astro-ph.CO]. [Erratum: Phys. Rev. D 90(7), 079902 (2014)]
16. XENON100 Collaboration, E. Aprile et al., Limits on spin-dependent WIMP-nucleon cross sections from 225 live days of XENON100 data. Phys. Rev. Lett. **111**(2), 021301 (2013). arXiv:1301.6620 [astro-ph.CO]
17. M. Baak, M. Goebel, J. Haller, A. Hoecker, D. Kennedy, R. Kogler, K. Moenig, M. Schott, J. Stelzer, The electroweak fit of the standard model after the discovery of a new boson at the LHC. Eur. Phys. J. C **72**, 2205 (2012). arXiv:1209.2716 [hep-ph]
18. Heavy Flavor Averaging Group Collaboration, Y. Amhis et al., Averages of B-Hadron, C-Hadron, and tau-lepton properties as of early 2012. arXiv:1207.1158 [hep-ex]
19. K. De Bruyn, R. Fleischer, R. Knegjens, P. Koppenburg, M. Merk, A. Pellegrino, N. Tuning, Probing new physics via the $B_s^0 \to \mu^+\mu^-$ effective lifetime. Phys. Rev. Lett. **109**, 041801 (2012). arXiv:1204.1737 [hep-ph]

20. LHCb, CMS Collaboration, V. Khachatryan et al., Observation of the rare $B_s^0 \to \mu^+\mu^-$ decay from the combined analysis of CMS and LHCb data. Nature **522**, 68–72 (2015). arXiv:1411.4413 [hep-ex]
21. CKMfitter Group Collaboration, J. Charles, A. Hocker, H. Lacker, S. Laplace, F.R. Le Diberder, J. Malcles, J. Ocariz, M. Pivk, L. Roos, CP violation and the CKM matrix: assessing the impact of the asymmetric B factories. Eur. Phys. J. C **41**, 1–131 (2005). arXiv:hep-ph/0406184 [hep-ph]
22. BaBar Collaboration, B. Aubert et al., A Search for $B^+ \to \ell^+\nu_\ell$ recoiling against $B^- \to D^0\ell^-\bar{\nu}X$. Phys. Rev. D **81**, 051101 (2010). arXiv:0912.2453 [hep-ex]
23. Belle Collaboration, K. Hara et al., Evidence for $B^- -> \tau^-\bar{\nu}$ with a semileptonic tagging method. Phys. Rev. D **82**, 071101 (2010). arXiv:1006.4201 [hep-ex]
24. BaBar Collaboration, J.P. Lees et al., Evidence of $B^+ \to \tau^+\nu$ decays with hadronic B tags. Phys. Rev. D **88**(3), 031102 (2013). arXiv:1207.0698 [hep-ex]
25. Belle Collaboration, I. Adachi et al., Evidence for $B^- \to \tau^-\bar{\nu}_\tau$ with a hadronic tagging method using the full data sample of Belle. Phys. Rev. Lett. **110**(13), 131801 (2013). arXiv:1208.4678 [hep-ex]
26. A. Czarnecki, W.J. Marciano, A. Vainshtein, Refinements in electroweak contributions to the muon anomalous magnetic moment. Phys. Rev. D **67**, 073006 (2003). arXiv:hep-ph/0212229 [hep-ph]. [Erratum: Phys. Rev. D 73, 119901 (2006)]
27. Muon g-2 Collaboration, G.W. Bennett et al., Measurement of the negative Muon anomalous magnetic moment to 0.7 ppm. Phys. Rev. Lett. **92**, 161802 (2004). arXiv:hep-ex/0401008 [hep-ex]
28. Muon g-2 Collaboration, G.W. Bennett et al., Final report of the Muon E821 anomalous magnetic moment measurement at BNL. Phys. Rev. D **73**, 072003 (2006). arXiv:hep-ex/0602035 [hep-ex]
29. A. Nyffeler, Hadronic light-by-light scattering in the muon g-2: a new short-distance constraint on pion-exchange. Phys. Rev. D **79**, 073012 (2009). arXiv:0901.1172 [hep-ph]
30. K. Hagiwara, R. Liao, A.D. Martin, D. Nomura, T. Teubner, $(g-2)_\mu$ and alpha(M_Z^2) re-evaluated using new precise data. J. Phys. **G38**, 085003 (2011). arXiv:1105.3149 [hep-ph]
31. T. Aoyama, M. Hayakawa, T. Kinoshita, M. Nio, Complete tenth-order QED contribution to the Muon g-2. Phys. Rev. Lett. **109**, 111808 (2012). arXiv:1205.5370 [hep-ph]
32. S. Heinemeyer, O. Stal, G. Weiglein, Interpreting the LHC Higgs search results in the MSSM. Phys. Lett. B **710**, 201–206 (2012). arXiv:1112.3026 [hep-ph]
33. ATLAS, CMS Collaboration, G. Aad et al., Combined measurement of the Higgs boson mass in pp collisions at $\sqrt{s} = 7$ and 8 TeV with the ATLAS and CMS experiments. Phys. Rev. Lett. **114**, 191803 (2015). arXiv:1503.07589 [hep-ex]
34. ATLAS Collaboration, M. Aaboud et al., Search for squarks and gluinos in final states with jets and missing transverse momentum at $\sqrt{s} = 13$ TeV with the ATLAS detector. Eur. Phys. J. C **76**(7), 392 (2016). arXiv:1605.03814 [hep-ex]
35. ATLAS Collaboration, Further searches for squarks and gluinos in final states with jets and missing transverse momentum at $\sqrt{s}$ =13 TeV with the ATLAS detector. Tech. Rep. ATLAS-CONF-2016-078, CERN, Geneva, Aug, 2016. https://cds.cern.ch/record/2206252
36. ATLAS Collaboration, G. Aad et al., Search for gluinos in events with an isolated lepton, jets and missing transverse momentum at $\sqrt{s}$ = 13 TeV with the ATLAS detector. Eur. Phys. J. C **76**(10), 565 (2016). arXiv:1605.04285 [hep-ex]
37. ATLAS Collaboration, Search for squarks and gluinos in events with an isolated lepton, jets and missing transverse momentum at $\sqrt{s}$ = 13 TeV with the ATLAS detector. Tech. Rep. ATLAS-CONF-2016-054, CERN, Geneva, Aug, 2016. https://cds.cern.ch/record/2206136
38. ATLAS Collaboration, G. Aad et al., Search for pair production of gluinos decaying via stop and sbottom in events with b-jets and large missing transverse momentum in pp collisions at $\sqrt{s} = 13$ TeV with the ATLAS detector. Phys. Rev. D **94**(3), 032003 (2016). arXiv:1605.09318 [hep-ex]
39. ATLAS Collaboration, Search for pair production of gluinos decaying via top or bottom squarks in events with b-jets and large missing transverse momentum in pp collisions at $\sqrt{s} = 13$ TeV with the ATLAS detector. Tech. Rep. ATLAS-CONF-2016-052, CERN, Geneva, Aug, 2016. https://cds.cern.ch/record/2206134
40. ATLAS Collaboration, Search for the supersymmetric partner of the top quark in the Jets+Emiss final state at sqrt(s) = 13 TeV. Tech. Rep. ATLAS-CONF-2016-077, CERN, Geneva, Aug, 2016. https://cds.cern.ch/record/2206250
41. ATLAS Collaboration, M. Aaboud et al., Search for top squarks in final states with one isolated lepton, jets, and missing transverse momentum in $\sqrt{s} = 13$ TeV pp collisions with the ATLAS detector. Phys. Rev. D **94**(5), 052009 (2016). arXiv:1606.03903 [hep-ex]
42. ATLAS Collaboration, Search for top squarks in final states with one isolated lepton, jets, and missing transverse momentum in $\sqrt{s}$ = 13 TeV pp collisions with the ATLAS detector. Tech. Rep. ATLAS-CONF-2016-050, CERN, Geneva, Aug, 2016. https://cds.cern.ch/record/2206132
43. Search for direct top squark pair production in final states with two leptons in $\sqrt{s} = 13$ TeV pp collisions using 3.2 fb^{-1} of ATLAS data. Tech. Rep. ATLAS-CONF-2016-009, CERN, Geneva, Mar, 2016. https://cds.cern.ch/record/2139643
44. ATLAS Collaboration, M. Aaboud et al., Search for bottom squark pair production in protonproton collisions at $\sqrt{s} = 13$ TeV with the ATLAS detector. Eur. Phys. J. C **76**(10), 547 (2016). arXiv:1606.08772 [hep-ex]
45. ATLAS Collaboration, M. Aaboud et al., Search for new phenomena in final states with an energetic jet and large missing transverse momentum in pp collisions at $\sqrt{s} = 13$ TeV using the ATLAS detector. Phys. Rev. D **94**(3), 032005 (2016). arXiv:1604.07773 [hep-ex]
46. B. Allanach, SOFTSUSY: a program for calculating supersymmetric spectra. Comput. Phys. Commun. **143**, 305–331 (2002). arXiv:hep-ph/0104145 [hep-ph]
47. A. Djouadi, M.M. Muhlleitner, M. Spira, Decays of supersymmetric particles: the program SUSY-HIT (SUspect-SdecaY-Hdecay-InTerface). Acta Phys. Polon. B **38**, 635–644 (2007). arXiv:hep-ph/0609292 [hep-ph]
48. T. Sjostrand, S. Mrenna, P.Z. Skands, A brief introduction to PYTHIA 8.1. Comput. Phys. Commun. **178**, 852–867 (2008). arXiv:0710.3820 [hep-ph]
49. DELPHES 3 Collaboration, J. de Favereau et al., DELPHES 3, a modular framework for fast simulation of a generic collider experiment. JHEP**1402**, 057 (2014). arXiv:1307.6346 [hep-ex]
50. Expected performance of the ATLAS b-tagging algorithms in Run-2. Tech. Rep. ATL-PHYS-PUB-2015-022, CERN, Geneva, Jul, 2015. http://cds.cern.ch/record/2037697
51. https://twiki.cern.ch/twiki/bin/view/LHCPhysics/SUSYCrossSections
52. A.L. Read, Presentation of search results: the CLs technique. J. Phys. G Nucl. Part. Phys. **28** (10), 2693 (2002). http://stacks.iop.org/0954-3899/28/i=10/a=313
53. A search for supersymmetry in events containing a leptonically decaying Z boson, jets and missing transverse momentum in $\sqrt{s} = 13$ TeV pp collisions with the ATLAS detector. Tech. Rep. ATLAS-CONF-2015-082, CERN, Geneva, Dec, 2015. https://cds.cern.ch/record/2114854